



- mFUSE: an interface for the graphical assembly of custom SHM processes
- Test structure data sets for benchmarking SHM algorithms

The SHMTools is the beginning of a larger effort to collect, archive, and share various approaches to SHM and can be downloaded from <http://institute.lanl.gov/ei/software-and-data/SHMTools/>. In this study, this software tool is used for SHM of a fitting lug assembly and sensor diagnostics in the presence of temperature variations.

### 3. Test structure: a UAV lug assembly

A lug joint is one of the most critical structural elements in aerospace applications. The lug assembly is fabricated from 25-mm thick Al 7075-T651 plate, 375 x 270 mm, shown in Figure 2. One side of this structure is bonded with a composite plate using 10 bolted joints at the torque level of 220 in-lb. The typical failure modes for this lug-assembly were identified as a fatigue crack at the tip of the lug and the wing, the loosening mode of joint failure, and fatigue crack initiation at bolt holes. Total 10 piezoelectric transducers (five 12.7-mm diameter and five 6.3-mm diameter) were installed on one surface of the lug as shown in the figure 2

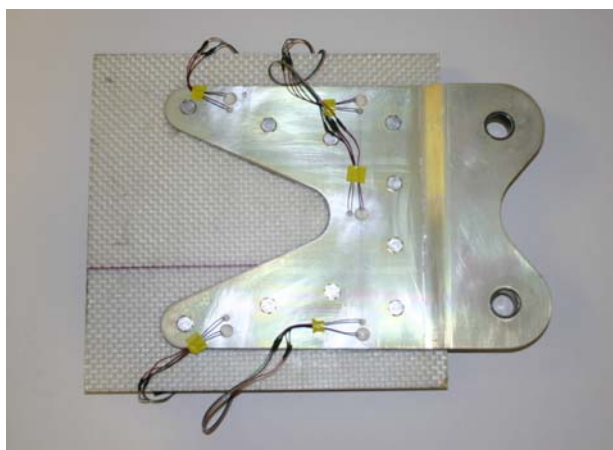


Figure 2. A lug assembly

### 4. SHM Procedure

It is a well known fact that frequency response functions (FRFs) represents a unique dynamic characteristic of a structure. From the standpoint of SHM, damage will alter the stiffness, mass, or energy dissipation properties of a system, which, in turn, results in the changes in the FRF<sup>2</sup>.

Additionally, time series predictive models, such as autoregressive model with exogenous inputs (ARX), can be used as a damage-sensitive feature extractor. An ARX model is fit to the data to capture the input/output relationship, which is intended to enhance the damage detection process by utilizing a piezoelectric active-sensing system<sup>3</sup>. Both techniques are applied to a lug assembly. Without any temperature changes, these methods could clearly identify structural damage, which was simulated by loosening connection bolts of the lug assembly<sup>4</sup>. In order to understand the effects of temperature variations on the damage detection capability, different temperature conditions were imposed to the structure in the range of 75-120F. The frequency response functions and time series data were measured at each stage of temperature and the damage condition was imposed in sequent as follows.

- D1: loosening one bolt to 100 in-lb,
- D2: to 20 in-lb
- D3: loosening two bolts to 100 in-lb,
- D4: to 20 in-lb

Similar temperature variations (75-100F) were also imposed into these damaged conditions.

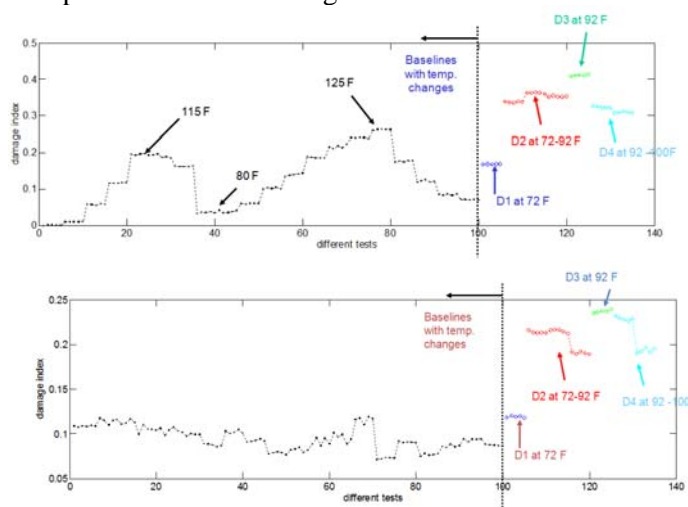


Figure 3. The SHM results using FRF measurements and SHMTools. The first figure shows the result that the baseline training data do not include temperature variations, while the second figure includes the variation.

Figure 3 show a correlation-based damage metric chart. The damage metric chart is constructed after each measurement has been taken in order to give some indication of the conditions of a structure

through comparison with the reference measurement. As can be seen in the figure, the effects of temperature on the FRF measurements were remarkable that the first damage state (D1) could not be clearly identifiable. However, from the second damage state (D2: loosening a bolt to 20 in-lb) introduced noticeable changes in FRF signature and could be clearly identified. If one uses all the temperature variation to baseline training data, the result is made clearly improved.

In addition to FRFs, SHM techniques based on time series predictive models were also implemented. It was however concluded that the residual error, which is the difference between the measured and the ARX predicted signal, was not suitable damage indicator, as shown in Figure 4. With the induced temperature variations, the residual error increases which makes impossible to distinguish the damaged condition from undamaged ones.

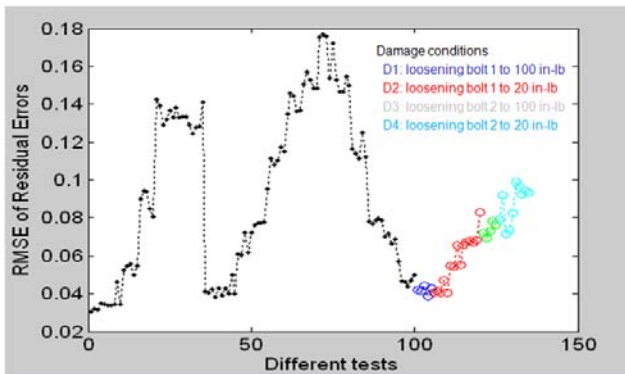


Figure 4. RMSE of residual error. Large increase in the residual error that damage could not be identifiable.

However, the statistical analysis on the identified AR and X parameters shows the much better damage detection capability. Figure 5 shows the AR parameters projected onto the first two principle components. Principle component analysis (PCA) is a classical linear technique of multivariate statistics for mapping multidimensional data into lower dimension with minimal loss of information. In SHM, PCA has been used for several purposes (evaluation of patterns, feature cleansing, feature selection), herein it is used only for feature visualization. The visualization of these parameters in the transformed space shows that each state condition clusters well in such a way that the

baselines along with temperature variations are linearly separable from the damaged conditions in the two-dimensional projection.

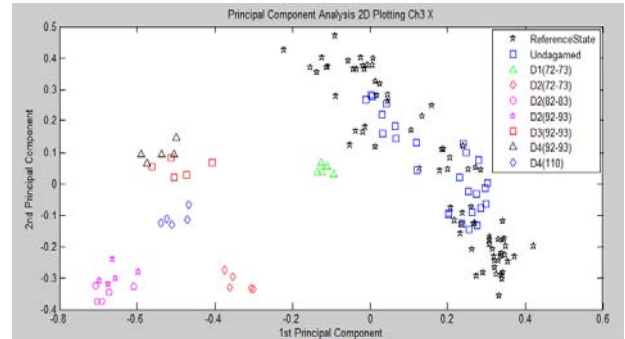


Figure 5. PCA projection of AR parameters. The separation of damaged and undamaged conditions are clearly observed.

Figure 6 illustrates the Mahalanobis squared distance-based damage metric values. The first 70 baselines in the temperature range of 80-125 F were included in the training set and the remaining data are used for damage identification. The figure clearly suggests that the Mahalanobis distance provides a clear damage indicator that can discriminate the damaged conditions from undamaged conditions in the presence of temperature variations.

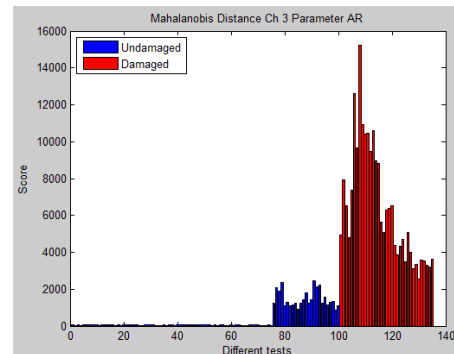


Figure 6. Mahalanobis squared distance using the AR parameters

It should be emphasized that the aforementioned SHM data processing techniques are embedded in the SHMTools software, and can be easily assembled. By integrating various data interrogation and signal processing algorithms, this powerful SHM tool enhances the visibility and interpretation of SHM methods related to damage identification

and can be applied to a wide variety of SHM applications.

### 5. Sensor Diagnostic Procedure

The sensor diagnostic process is one of the most important SHM components as, if there is a response change, one must be able to identify that the change is caused by structural damage or just from a sensor failure. The basis of this method is to track the capacitive value of PZT transducers, which manifests in the imaginary part of the measured electrical admittance. Both degradation of the mechanical/ electrical properties of a PZT transducer and the bonding defects between a PZT patch and a host structure can be identified by the proposed process<sup>5</sup>. However, it was found that temperature variations in sensor boundary conditions manifest themselves in similar ways in the measured electrical admittances, which imposed difficulties in sensor diagnostics in the presence of temperature variations. Therefore, an efficient signal processing tool was developed<sup>6</sup> that enables the identification of a sensor validation feature that can be obtained instantaneously without relying on pre-stored baselines, and is not affected by temperature variations. This process is embedded into the SHMtools.

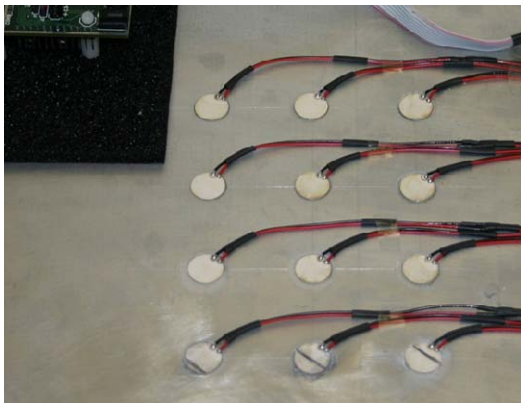


Figure 7. Sensor Diagnostics plate with healthy, debonded, and broken sensors

For the test, twelve circular piezoelectric patches are mounted using super-glue on one surface of an Aluminum plate (30 x 30 x 1.25 cm), shown in Figure 7. The size of the circular PZT patch is 5.5

mm diameter with 0.2 mm thickness. Patches had a different bonding condition, perfect bonding, debonding, and sensor breakages. Six patches were under perfect bonding condition, three of them were under the different degree of debonding conditions (25%, 50%, and 75% area debonding), and the remaining three were under different fracture conditions (25%, 50%, and 75%). Admittance measurements in the frequency range of 5-30 kHz were made to each PZT patch. The temperature variation in the range of 70-140 F was also imposed to this structure.

When the baseline and damaged sensors were measured at the same temperature, the sensor diagnostic technique could detect the broken or debonded sensors without giving any false indication. However, if a more than 45F temperature difference exists between the baseline measurement and the undamaged sensor, then 25% broken or debonded sensors were not clearly detected. Other failure conditions were clearly detected with the proposed technique even with this degree of temperature variations.

In order to simulate more realistic conditions, the baseline sensors were measured at slightly different temperature and the same sensor diagnostic process was applied. Figure 8 shows one of the examples. As can be seen, the 50% broken sensor measured at 86F could be detected when each baseline sensor was measured in the temperature range of 72-91F. 25% debonded or broken sensors were also detected with only a few false indication.

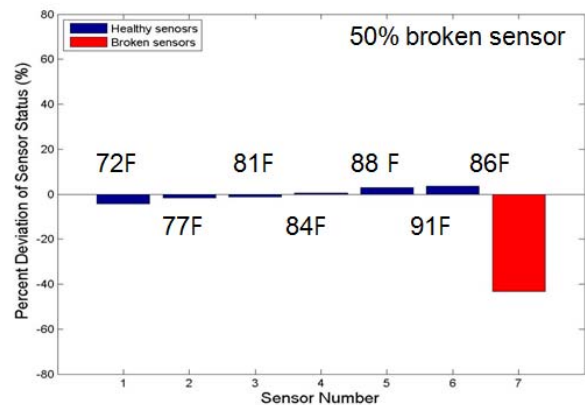


Figure 8. Sensor Diagnostics result of a 50% broken sensor with mixed baseline temperature.



## **6. Conclusion**

The results collected from the tests shows that SHMTools can be efficiently used for identifying a common failure mode of a lug assembly and monitoring the functionality of SHM sensors. The use of SHMTools can provide a certain advantage as the software allows the user to easily assemble and embed any SHM process. Several data normalization processes are also embedded in SHMtools for both SHM and sensor diagnostics and experimentally demonstrated in this paper.

Validation Using Instantaneous Baseline Data,” IEEE Sensors Journal, Vol.9, No.11, pp. 1414-1421.

## **Acknowledgement**

This research was supported by Basic Science Research Program through the National Research Foundation of Korea funded by the Ministry of Education, Science and Technology (2011-0010489) and partially supported by Korea Ministry of Land, Transport and Maritime Affairs as Haneul Project.

## **References**

- [1] Flynn, E.B., Kpotufe, S., Dondi, D., Figueiredo, E.F., Mollov, T., Todd, M.D., Rosing, T.S., Taylor, S.G., Park, G., Farrar, C.R., “SHMTools: A new embeddable software for SHM applications” *Proceedings of 17<sup>th</sup> SPIE Conference on Smart Structures and Nondestructive Evaluation*, March 7-11 2010, San Diego, CA.
- [2] Park, G., Rutherford, C.A., Wait, J.R., Nadler, B.R., Farrar, C.R., 2005, “The Use of High Frequency Response Functions for Composite Plate Monitoring with Ultrasonic Validation,” *AIAA Journal*, Vol. 43, No. 11, pp. 2431-2437.
- [3] Figueiredo, E., Park, G., Farinholt, K.M., Farrar, C.R., “Time Series Analyses of Piezoelectric Active-sensing for Structural Health Monitoring Applications,” *Journal of Vibration and acoustics*.
- [4] Park, G., Park, C.Y., Jun, S.M., Farrar, C.R., “Monitoring of Bolted Joints using Piezoelectric Active-Sensing for Aerospace Applications,” *Proceedings of 5th European Structural Health Monitoring Conference*, June 29-July 2 2010, Sorrento, Naples-Italy.
- [5] G. Park, C. R. Farrar, F. Lanza di Scalea, S. Coccia, “Performance Assessment and Validation of Piezoelectric Active Sensors in Structural Health Monitoring,” *Smart Materials and Structures*, Vol. 16, No. 6, pp. 1673-1683, 2006.
- [6] Overly, T.G., Park, G., Farinholt, K.M., Farrar, C.R., 2009. “Piezoelectric Active-Sensor Diagnostics and